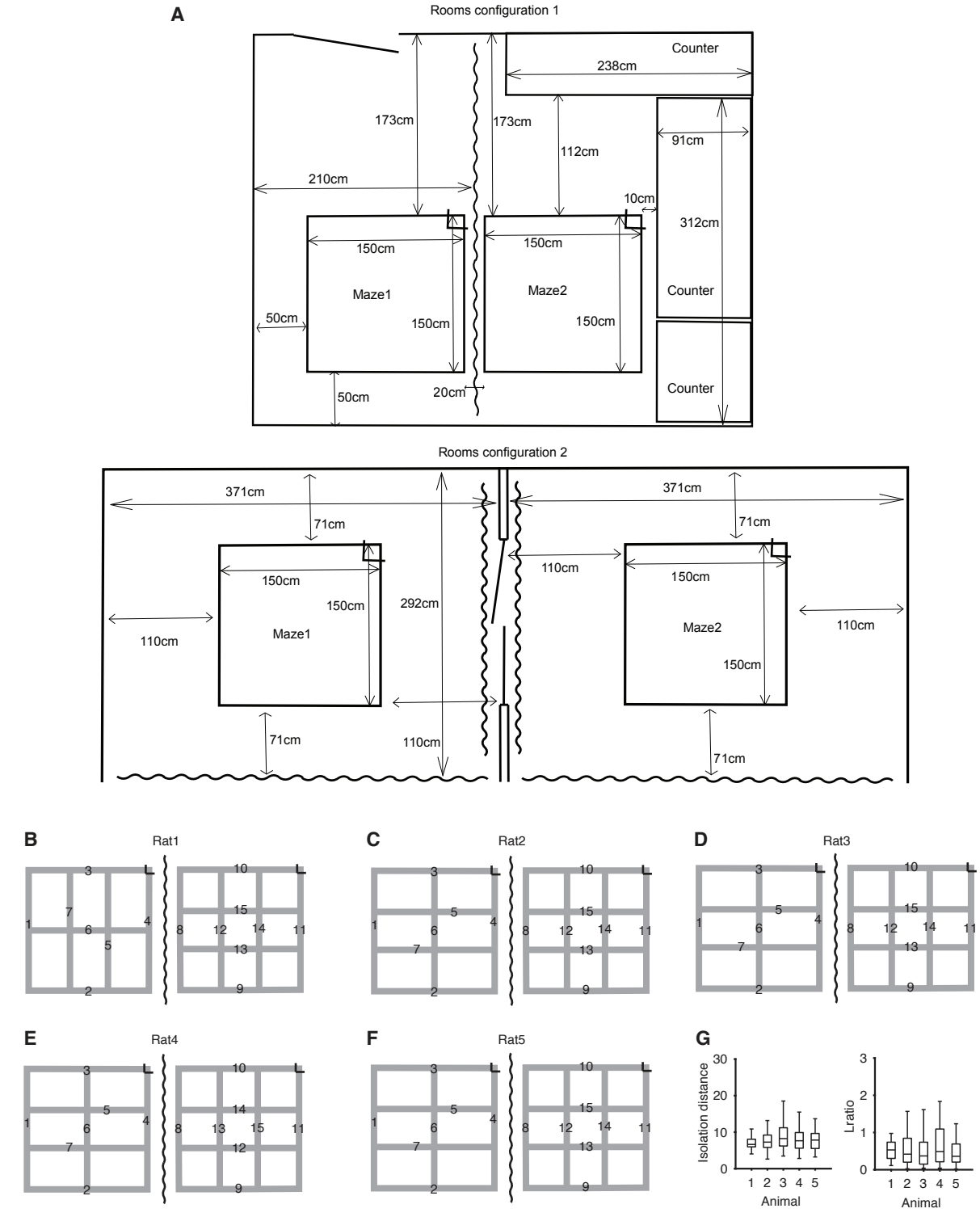

Figure S1. Experiment design. Related to Figure 1.

(A) Diagram of the two mazes and rooms configuration. Rats 1-4 were recorded in the top room configuration, Rat 5 in the bottom room configuration. The sleep box was located within the perimeter of Maze1 in Room1 and was removed from the rooms for the duration of the run sessions. (B-F) The diagram of mazes and location of each track in each animal. (G) Isolation distance and L-ratio of spike clusters for the entire 16 h-long recording day.

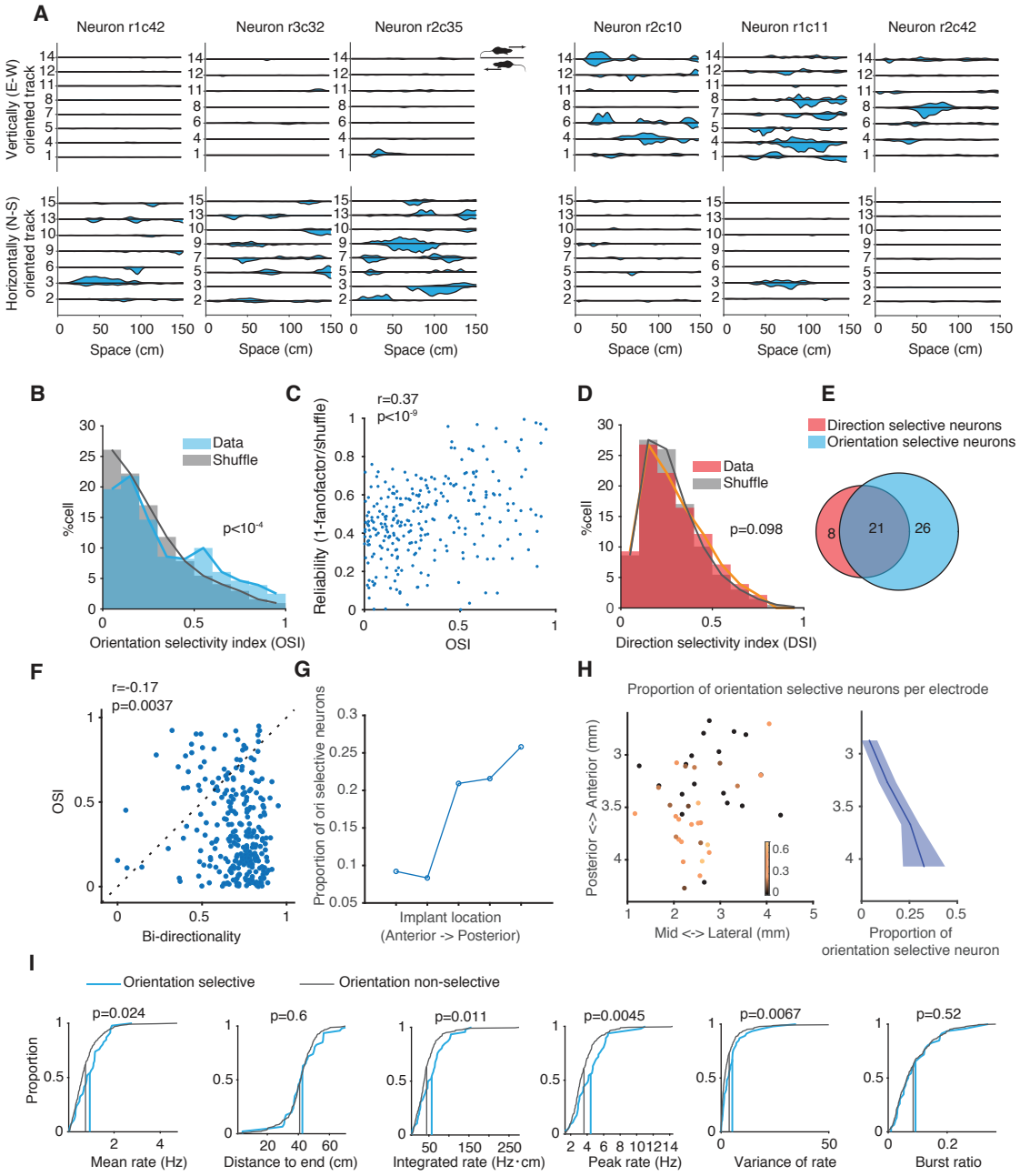

Figure S2. Orientation selectivity of neurons. Related to Figure 2.

(A) Examples of orientation selective neurons. (B) Distribution of orientation selectivity index (OSI) in the neuronal population. (C) Reliability of the OSI quantified by the Fano factor. (D) Distribution of direction selectivity index (DSI) in the neuronal population. (E) Relationship between orientation selective and direction selective neurons. (F) Relationship between neuronal bidirectionality of firing during run on linear tracks and OSI. (G) Proportion of orientation selective neurons in each animal sorted according to the location of their corresponding electrode recording site in the hippocampus. (H) Relationship between the proportion of orientation selective neurons in each electrode and electrode location. (I) Comparison between place map properties of orientation selective and non-selective neurons. Place maps of orientation selective neurons have higher mean, peak, and integrated firing rates and higher variance of rates compared with the non-selective neurons. Data are represented as mean±SEM.

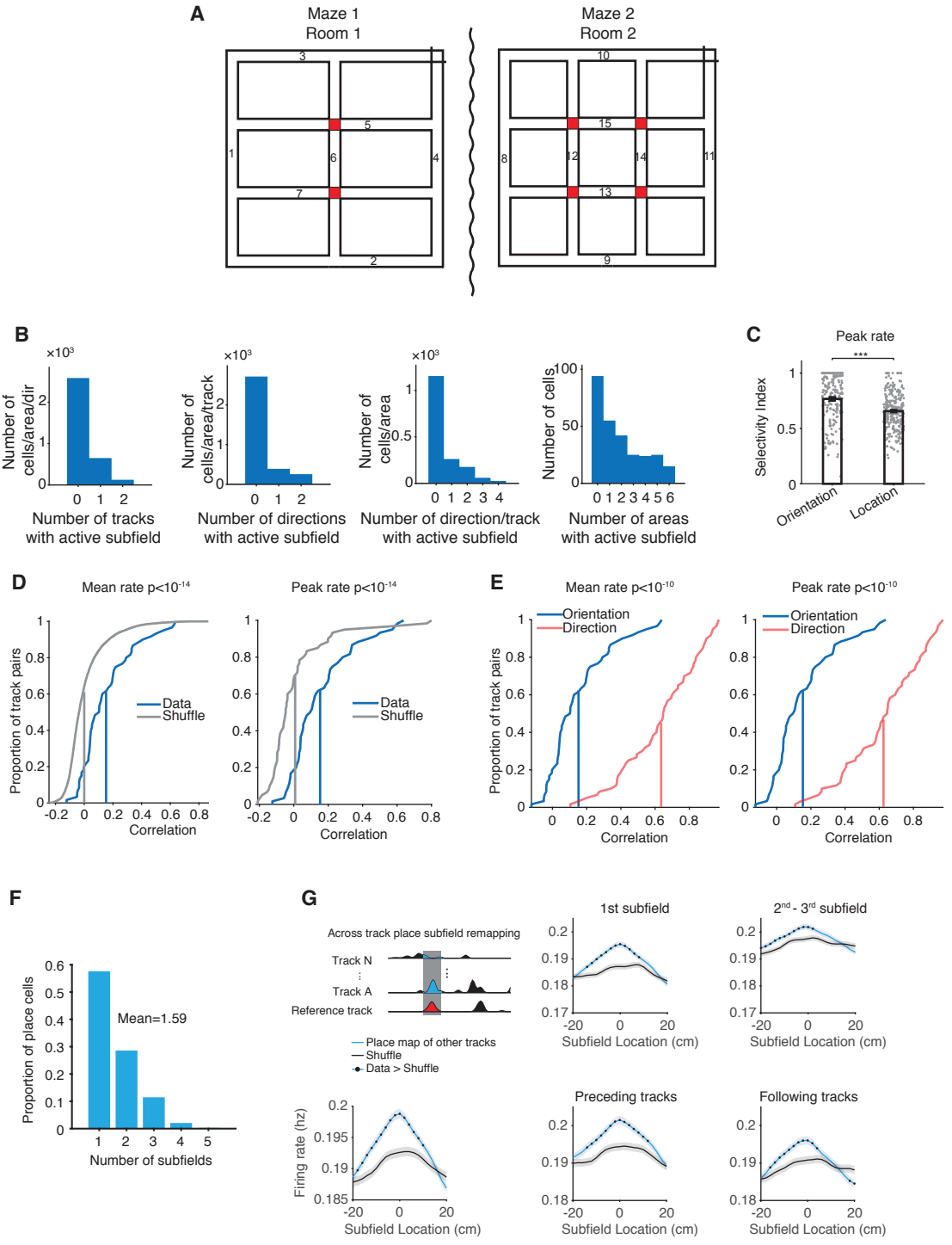

Figure S3. Place maps in intersectional areas and place subfield remapping. Related to Figure 3.

(A) Illustration of non-rewarded inner tracks intersectional areas. (B) Statistics of place cell responses in intersectional areas. (C) Orientation selectivity inside intersectional areas and location selectivity on the same track calculated by peak firing rate. (D) Correlation of population response mean (Left) or peak rate (Right) during runs along the same orientations in intersectional areas. Vertical bars represent mean values. (E) Correlation of population mean (Left) or peak rate (Right) during runs along the same orientations compared with along the same direction in intersectional areas. Vertical bars represent mean values. (F) Distribution of the number of place subfields among all place cells. (G) Average firing rate of place subfield activity on other tracks extracted in locations topologically corresponding to the reference track, separated by primary (peak firing rate) subfields and secondary-tertiary subfields, and the order of exploration in relation to the reference track (preceding or following). Data are represented as mean±SEM. ***P < 0.001.

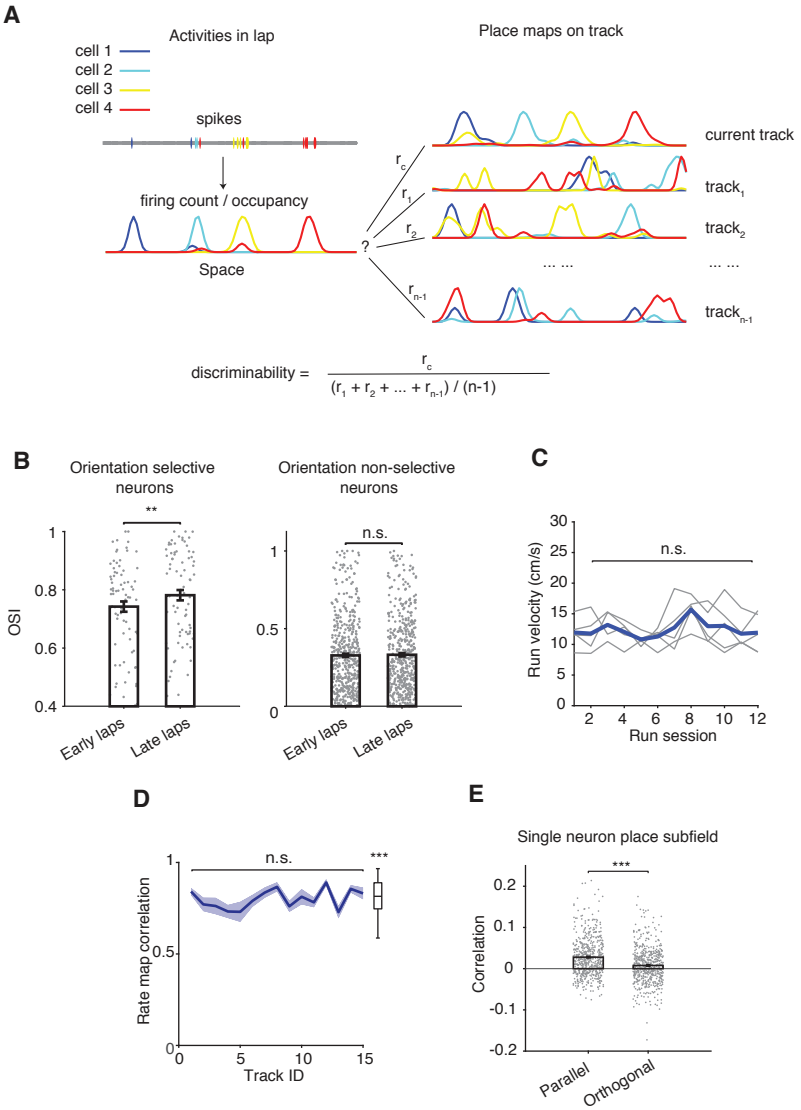

Figure S4. Temporal dynamics of track discrimination. Related to Figure 4.

(A) Diagram of the method used to calculate track discriminability. Only 4 neurons (color-coded) are shown here for illustration clarity. (B) OSI of orientation selective neurons (left) and orientation non-selective neurons (right) in early laps and late laps. (C) Animal velocity across individual run sessions. (D) Rate map correlation between the first half and second half of each session across all tracks. Boxplot is the average of all tracks (mean±SEM=0.8±0.009). (E) Correlation of single neuron place map between parallel tracks or between orthogonal tracks. Data are represented as mean±SEM. *P < 0.05, ***P < 0.001, n.s., not significant.

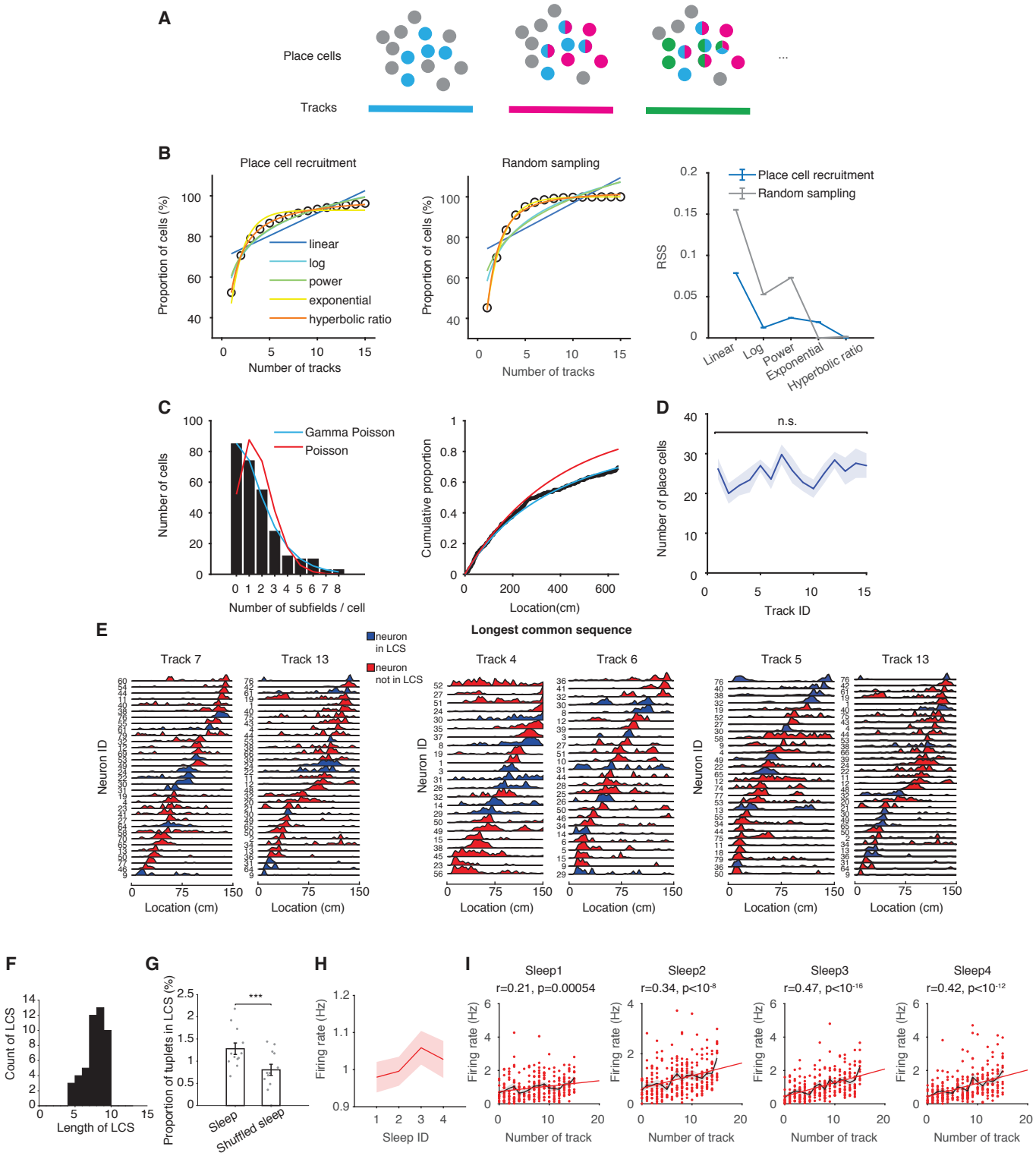

Figure S5. Place cell recruitment and remapping across the fifteen tracks. Related to Figure 5.

(A) Methodological diagram of place cell recruitment across multiple tracks emphasizing that neurons are re-used as place cells across multiple tracks. (B) Place cell recruitment curve fitted by multiple candidate functions. RSS: residual sum of squares. Lower RSS signifies better fit. (C) Distribution of place subfields (left) and of number of tracks/cell (right) in the 6 m-long continuous runs (tracks 1-4 and tracks 8-11) fitted by a Poisson model or a Gamma Poisson model (best fit). (D) Number of place cells on each track averaged across all animals. (E) Example of neuronal longest common sequence (LCS, place cells in blue color) across three track pairs. (F) Distribution of number of neurons in the LCS across track pairs. (G) Participation of neuronal tuplets from sleep sequences into LCSs across run sequences. (H) Average neuronal firing rates during the 4 sleep sessions. (I) Neurons' firing rates during sleep sessions as a function of the number of tracks on which they expressed place subfields. Data are represented as mean±SEM. n.s., not significant. ***P < 0.001.

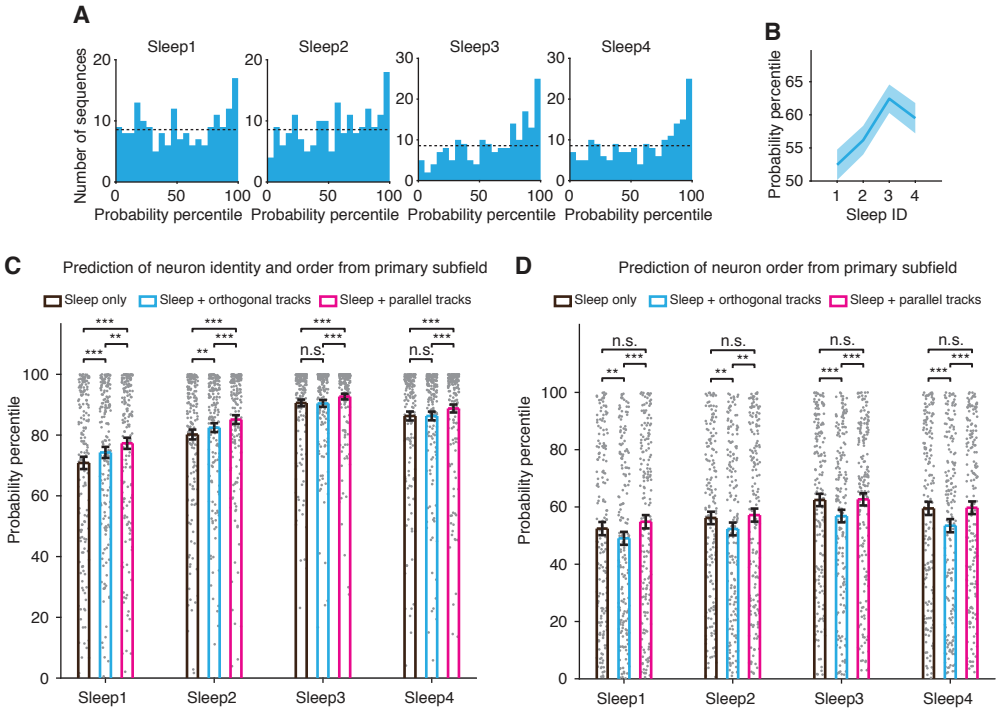

Figure S6. Inferred likelihood of run sequences computed from sleep and from combined sleep and runs on different tracks using a first order Markov chain model. Related to Figure 6.

(A) Markov chain model-based inferred probability percentile of neuronal order during run sequences computed from each sleep session. Horizontal dotted line represents chance distribution. (B) Markov model-based inferred probability percentile of neuronal order during run sequences from activity during sleep as a function of sleep ID. (C-D) Changes in the Markov chain model-based inferred probability percentile of neuronal identity and order (C) and neuronal order (D) during run when Markov model was based only on primary subfields from combined sleep and run sequences on other tracks compared with sleep only. Data are represented as mean±SEM. **P < 0.01, ***P < 0.001, n.s., not significant.